Cell Death and Differentiation (2013) 20, 1546–1557

www.nature.com/cdd

Potent and multiple regulatory actions of microglial glucocorticoid receptors during CNS inflammation

MÁ Carrillo-de Sauvage[1,2,3,4], L Maatouk[1,2,3], I Arnoux[5,6], M Pasco[1,2,3], A Sanz Diez[5,6], M Delahaye[1,2,3], MT Herrero[4], TA Newman[7], CF Calvo[8], E Audinat[5,6], F Tronche[1,2,3] and S Vyas*[,1,2,3]

In CNS, glucocorticoids (GCs) activate both GC receptor (GR) and mineralocorticoid receptor (MR), whereas GR is widely expressed, the expression of MR is restricted. However, both are present in the microglia, the resident macrophages of the brain and their activation can lead to pro- or anti-inflammatory effects. We have therefore addressed the specific functions of GR in microglia. In mice lacking GR in macrophages/microglia and in the absence of modifications in MR expression, intraparenchymal injection of lipopolysaccharide (LPS) activating Toll-like receptor 4 signaling pathway resulted in exacerbated cellular lesion, neuronal and axonal damage. Global inhibition of GR by RU486 pre-treatment revealed that microglial GR is the principal mediator preventing neuronal degeneration triggered by lipopolysaccharide (LPS) and contributes with GRs of other cell types to the protection of non-neuronal cells. *In vivo* and *in vitro* data show GR functions in microglial differentiation, proliferation and motility. Interestingly, microglial GR also abolishes the LPS-induced delayed outward rectifier currents by downregulating Kv1.3 expression known to control microglia proliferation and oxygen radical production. Analysis of GR transcriptional function revealed its powerful negative control of pro-inflammatory effectors as well as upstream inflammatory activators. Finally, we analyzed the role of GR in chronic unpredictable mild stress and aging, both known to prime or sensitize microglia *in vivo*. We found that microglial GR suppresses rather than mediates the deleterious effects of stress or aging on neuronal survival. Overall, the results show that microglial GR acts on several key processes limiting pro-inflammatory actions of activated microglia.
Cell Death and Differentiation (2013) **20,** 1546–1557; doi:10.1038/cdd.2013.108; published online 6 September 2013

Microglia as primary sensors of danger signals or of altered microenvironment rapidly undergo a programmed molecular and morphological transformation to elicit an inflammatory response.[1] In the CNS, microglial-mediated inflammatory processes triggered by nerve injury, trauma, ischemia or pathogen invasion are often associated with cellular damage. However, initiation of an innate immune response and inflammatory reaction also entails activation of various regulatory controls that prevent inappropriate tissue damage and stimulate tissue repair processes, for example, phagocytosis, neovascularization, neurogenesis and synaptic plasticity.[2–4] Among the regulatory controls, mechanisms such as transcriptional and post-transcriptional repression of pro-inflammatory cytokines or neo-synthesis of anti-inflammatory molecules and inhibitors of inflammatory signaling pathways are known to attenuate the activated pro-inflammatory state of microglia. Nevertheless, it remains unclear how microglia regulate their different modes of actions including switching on and off the resting (surveying), inflammatory or reparative states on different insults.[5] In this respect, microglia are phenotypically described as heterogeneous related likely to their different functional responses as a result of specific changes in their immediate environment.[2]

The neuroendocrine system through activation of steroid hormone receptors, for example, glucocorticoid receptor (GR), mineralocorticoid receptor (MR) or estrogen receptor (ER), is known to exert powerful modulatory effects on immune responses.[6] Indeed, microglia express these ligand-dependent nuclear receptors.[7] Although their molecular actions during an inflammatory process triggered in glia, which affects neuronal survival, are beginning to be elucidated,[8,9] their exact functions in microglial physiology remain to be determined. In CNS, MR and GR are activated by

[1]Department of Physiopathology of CNS diseases, Centre National de la Recherche Scientifique, UMR 7224, Molecular Genetics, Neurophysiology and Behavior Lab, Paris, France; [2]Institut National de la santé et de la Recherche Médicale, UMR 952, Paris, France; [3]Université Pierre et Marie Curie, Paris, France; [4]Clinical and Experimental Neuroscience (NiCE-CIBERNED), School of Medicine, University of Murcia, Regional Campus of International Excellence 'Campus Mare Nostrum', Murcia, Spain; [5]Institut National de la santé et de la Recherche Médicale, U603, Paris, France; [6]Paris Descartes University, CNRS UMR 8154, Paris, France; [7]Department of Clinical Neurosciences, Faculty of Medicine, Life Sciences B85, University of Southampton, Southampton, UK and [8]INSERM U975, CNRS UMR 7225, UPMC, Centre de Recherche de l'Institut du Cerveau et de la Moelle Epinière, Paris, France
*Corresponding author: S Vyas,Pathophysiology of CNS Diseases, CNRS UMR 7224, INSERM U 952, UPMC, Neurophysiology and Behavior Lab, 9 Quai St. Bernard, Paris 75005, France. Tel: +33 144279135; Fax: +33 144276159; E-mail: sheela.vyas@snv.jussieu.fr
Keywords: microglia; glucocorticoid receptors; inflammation; neuron survival; LPS
Abbreviations: COX-2, cyclooxygenase-2; CUMS, chronic unpredictable mild stress; GFAP, glial fibrillar acidic protein; IFN-γ, interferon gamma; IL-1β, interleukin1-β; iNOS, inducible nitric oxide synthase; LPS, lipopolysaccharide; LFB, luxol fast blue; MCP-1, monocytes chemotactic protein-1; TLR4, Toll-like receptor 4; TNF-α, tumor necrosis factor-α
Received 22.11.12; revised 18.5.13; accepted 21.6.13; Edited by JA Cidlowski; published online 06.9.13

glucocorticoids (GCs) with different affinities, additionally MR can be activated by aldosterone in non-neuronal cells.[10] Whereas MR promotes pro-inflammatory effects,[11,12] GR acts to limit inflammation and stimulate the resolution phase;[13] recent studies, however, suggest that their actions in inflammation are complex as well as context dependent. Thus, for example, systemic administration of GR antagonist RU486 was shown to exacerbate cell damage initiated by a single intrastriatal injection of LPS[14] indicating important protective role of GR. However, increased GCs levels in response to different psychogenic stressors, such as restraint stress, unpredictable stress, repeated social defeat or inescapable shock, have been correlated with pro-inflammatory cytokine production and sensitization of microglia. Moreover, subsequent inflammatory triggers aggravate neuronal injury.[15–20] Finally, alterations in the HPA axis during aging can result in chronically high GC levels that are known to contribute to immunosenescence exemplified by a sustained low production of pro-inflammatory molecules.[21,22] Thus, depending on the context, GC-GRs appear to exert either pro- or anti-inflammatory actions.

In contrast to the well-studied actions of GC-GR in peripheral immune cells, the precise functions of GR in microglia, the CNS immune-responsive cells, remain poorly understood. In this study, using mice conditionally inactivated for GR gene in macrophages/microglia, we report hitherto unappreciated actions of GR in relation to acute inflammation as well as during aging and stress.

Results

Inactivation of GR gene in $GR^{LysMCre}$ mutant mice. The selective absence of microglia in $GR^{LysMCre}$ mice was verified by double immunofluorsecence analysis of GR with microglial, neuronal astroglial or oligodendroctye markers in striato-cortical regions (Supplementary Figures S1A–D). GR mRNA level in microglial cultures obtained from mutant was negligible (Supplementary Figure S1E). No compensatory changes in MR levels or local production of GCs by corticosterone-metabolizing enzymes 11-β hydroxysteroid dehydrogenases 1 and 2 that may be affecting the inflammatory state in mutants were found. ER alpha mRNA levels were similar in both genotypes (Supplementary Figure S1F). MR mRNA levels remained unaltered in the cortico-striatal lesioned region after LPS injection in control and mutant mice, by contrast GR showed diminution in the mutants (Figure 1e).

The absence of GR in microglia exacerbates inflammatory lesion and induces neuronal degeneration following a single intraparenchymal LPS injection. Cellular, axonal and neuronal damage resulting from a single injection of either saline or LPS in right striatal region was compared between $GR^{LysMCre}$ mice and control littermates. In both the groups, saline injection showed negligible cellular damage analyzed after 3 days by cresyl violet staining. However, LPS-induced cellular damage was significantly greater in mutants compared with controls; the lesion size being dependent on LPS dose ($P=0.02$ and 0.03 for 1.5 and 5 μg LPS, respectively, Figure 1a). As LPS-induced inflammation can damage axonal fibers and promote demyelination,[14] we analyzed myelinated axonal tracts in the corpus callosum using luxol fast blue (LFB) staining. The results of LFB at 3 days after 1.5 or 5 μg/μl LPS injection indicated that demyelination had occurred in the corpus callosum of $GR^{LysMCre}$ but not control mice. Lesion area in corpus callosum and peri-corpus callosum was significantly greater in mutants ($P=0.05$, Figure 1b). After 7 days, in both control and mutant mice, an accumulation of cells was observed in corpus callosum suggesting an ongoing repair process independent of microglial GR. To examine whether microglial GR has a role in regulating neuronal damage, degenerating neurons labeled with Fluoro-Jade B present mostly in the cortical area were quantified. In saline-injected control and mutant mice, only a few and similar number of Fluoro-jade B+ neurons were observed where the needle had pierced. In sharp contrast, following 1.5 μg/μl of LPS injection, the number of degenerating neurons increased two- to threefold in mutant but not control mice ($P=0.005$, $n=6$, Figure 1d) at 3 days returning to saline levels after 7 days (Figure 1d).

Circulating corticosterone levels increased four- to fivefold in both control and mutant mice 3 days after LPS compared with basal non-injected animals. The mutant group showed slightly higher level indicating that despite high corticosterone levels they sustained greater cellular damage from LPS-induced inflammatory reaction (Figure 1c).

Microglial GRs are the principal regulators of LPS-induced neuronal degeneration. To determine whether GR expressed in other cell types than microglia has a role in LPS-induced cellular damage, we injected mice intraperitoneally (i.p.) with GR antagonist RU486 16 h before LPS intrastriatal injection. In control mice, the cellular and axonal lesions were significantly greater after RU486 pre-treatment compared with vehicle-injected mice (Figures 2a and b). Interestingly, in mutant mice, a further significant increase in lesion was observed ($P=0.03$) strongly suggesting that the magnitude of inflammation is aggravated by inactivation of GR in microglia together with GR inhibition in other cells. In contrast, although RU486 pre-treatment augmented neuronal degeneration in control mice, no further increase was observed in mutants (Figure 2c). When mice were pre-treated for 4 h with RU486 to limit nonspecific secondary alterations and killed 24 h after LPS injection, mutants displayed similar increase in lesion with no difference in neuronal degeneration between the two genotypes (Figure 2d) indicating that microglia GRs are the sole mediators involved in the protection of neurons. As it is possible that invading immune cells may participate in inflammation-induced damage, we assessed the role of GR in T cells in GR^{LckCre} mice. No difference in total necrotic lesion, damage to corpus callosum or neuronal degeneration was observed between GR^{LckCre} and control mice (Supplementary Figures S2A–C).

Microglial GR regulates microglial proliferation, activation and motility. The reactive microglia and astroglia, assessed by F4/80 and glial fibrillar acidic protein (GFAP) immunofluorescence, respectively, were present in the cortex,

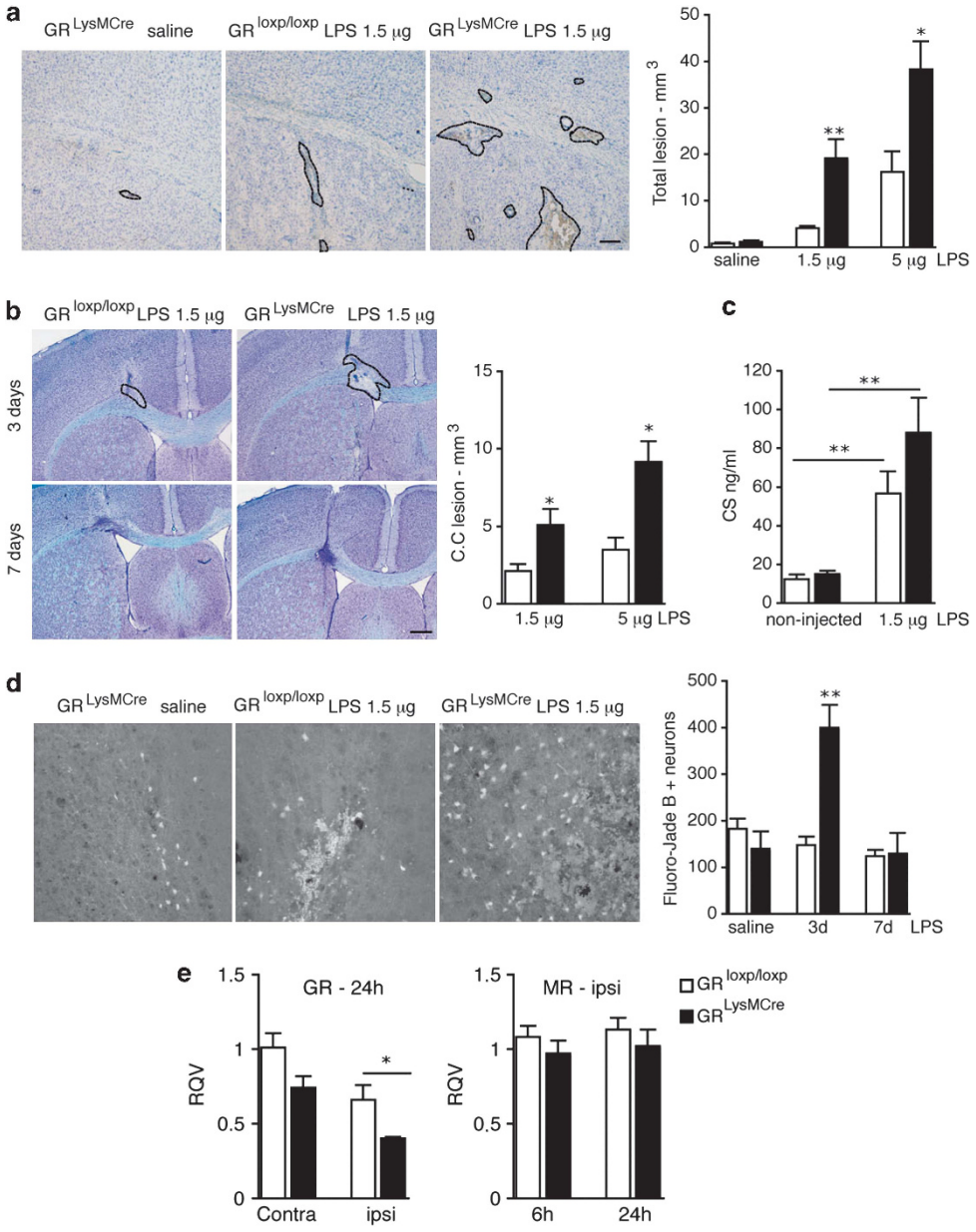

Figure 1 Analysis of cellular and neuronal lesion in $GR^{loxp/loxp}$ and $GR^{LysMCre}$ mice following a single intraparenchymal injection of LPS. (**a**) Panels depict representative examples of cresyl violet staining 3 days after a single injection of either 1 μl saline or 1.5 μg/μl LPS. The lesion size (depicted as broken lines) was quantified in control and mutant mice 3 days after saline or LPS. (**b**) Panels showing examples of LB and cresyl violet staining 3 or 7 days following 1.5 μg/μl LPS injection. Demyelination in corpus callosum is evident in $GR^{LysMCre}$ mice at 3 days; at 7 days appearance of cells at injured sites suggestive of ongoing reparative processes is observed in both controls and mutants. The graph depicts quantification of lesion in corpus callosum, $n = 4$–5 per group. $^{*}P \leq 0.05$ control *versus* $GR^{LysMCre}$ mice. (**c**) Systemic corticosterone levels in control and $GR^{LysMCre}$ mice, basal and 3 days following LPS injection. (**d**) Panels showing representative examples of Fluoro-Jade B staining in cortex after saline or LPS injection in control and mutant $GR^{LysMCre}$ mice. Fluoro-Jade B + cells were quantified, the results show significant neurodegeneration induced by LPS in $GR^{LysMCre}$ mice and no effect in controls. $n = 4$–5 per group. $^{**}P \leq 0.02$, $^{*}P \leq 0.05$ control *versus* $GR^{LysMCre}$ mice. Scale bar = 100 μm. (**e**) RT-qPCR measurement of GR (contra and ipsilateral sides) and MR mRNA levels in controls and mutants at times indicated after LPS injection. $^{**}P \leq 0.02$ control *versus* $GR^{LysMCre}$ mice, $n = 4$–5 per group

septum and striatum on the ipsilateral side of LPS injection. A greater number of microglial cells exhibited amoeboid morphology in the cortical and septal areas in $GR^{LysMCre}$ compared with control mice (Figure 3a). Measurement of the surface area showed that the reactive microglial area was almost double in the $GR^{LysMCre}$ ($P = 0.032$, Figure 3b). In contrast, no significant difference was observed in the reactive astroglial morphology or in the area between $GR^{LysMCre}$ and control mice (Figures 3b and c). BrDU incorporation revealed a clear increase in microglial but not astroglial proliferation in mutants ($P = 0.02$, Figure 3d).

***In vitro* microglia exhibit reduced motility and increased amoeboid morphology in the absence of GR.** The role of microglial GR in morphological and cell motility alterations that characterize their activation was analyzed by video

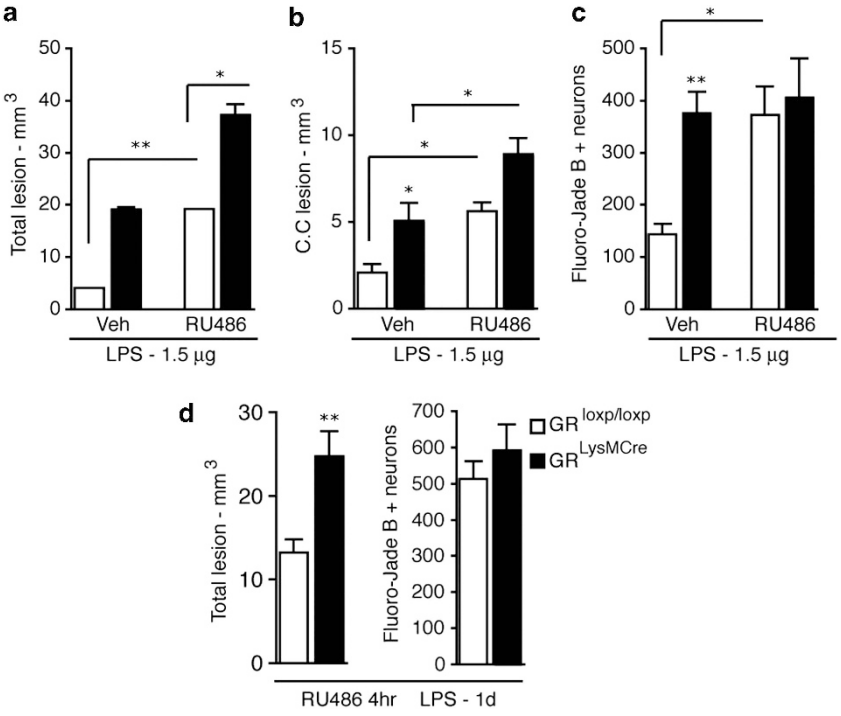

Figure 2 Examination of RU486 pre-treatment on injury triggered by injection of LPS. Control and $GR^{LysMCre}$ mice were either i.p. injected with DMSO or RU486 16 h before intraparenchymal LPS injection. Total cellular lesion (**a**) or in lesion corpus callosum (**b**) was quantified 3 days after LPS injection. RU486 pre-treatment augments LPS-induced lesion in control mice, which is exacerbated in $GR^{LysMCre}$ mice. (**c**) Quantification of Fluoro-Jade B + cells 3 days after LPS injection in DMSO or RU486 pre-treated mice shows that RU486 pre-treatment significantly augments the number of degenerating neurons in control mice and not in mutants. (**d**) Total cellular lesion and Fluoro-Jade B + cells in mice pre-treated withRU486 for 4 h and killed 24 h after LPS injection. $n = 4$–5 per group. $^{**}P \leq 0.02$, $^{*}P \leq 0.05$

microscopy in primary microglial cultures from P1 $GR^{LysMCre}$ and control pups. Majority of microglia in culture exhibit either rod-like or amoeboid morphology. Quantification of video-microscopic images taken every 10 min for a period of 10–15 h showed a greater percentage of $GR^{LysMCre}$ microglia exhibiting amoeboid morphology compared with control microglia and this feature remained unchanged with time (Figure 4b). To analyze cell movement, microglia were tracked on video-microscopic images (Figure 4a). Mean distance was calculated from four fields of each condition in duplicates (Figure 4c) or by cell migration assay using FluoroBlok inserts (Figure 4d). The tracking analyses showed that $GR^{LysMCre}$ microglia have drastically reduced capacity for motility ($P = 0.001$, number of cells = 20 to 26 from three experiments, paired *t*-test, Figure 4c). Cell movement of control microglia was significantly reduced by LPS treatment. As cell motility is ATP dependent, control but not mutant cultures treated with ATP inhibitor, Ox-ATP, had significantly reduced microglial motility ($P = 0.01$). Similar results were obtained in cell migration assay when fluorescence of $DiIC_{12}$ (3)-labeled cells that had migrated to the other side of the inserts was monitored at 2 and 4 h, with LPS reducing cell migration (Figure 4d).

GR regulates delayed outward rectifier currents induced by LPS by repressing the expression of $K_v1.3$ voltage-activated potassium channel. Microglia activation is associated with an induction of voltage-activated potassium channels of the delayed rectifier family, which regulate several functional properties of these cells, for example, proliferation and production of inflammatory molecules.[23] To test whether GR also modulates this aspect of microglia activation, we performed whole-cell recordings of cultured microglial cells. As previously observed[24] microglial cells recorded in control conditions expressed mostly inwardly rectifying potassium currents activated by hyperpolarization (data not shown) and barely detectable delayed rectifier outward currents activated by depolarization (Figure 5a). After 6 to 24 h of LPS treatment, large outward currents resembling potassium delayed rectifier currents were evoked by depolarizing steps above –30 mV ($P = 0.008$, Figure 5a). In the presence of dexamethasone (100 nM) during the LPS treatment, these outward currents were not observed during depolarizing steps ($P = 0.02$, Figures 5a and b), indicating that GR stimulation inhibits the induction of delayed rectifier currents by LPS.

We reasoned that Kv1.3 channel, reported to largely mediate this current in activated microglia,[23,25] could be a potential GR target as LPS was shown to stimulate its expression in cultured rat microglia.[26] Indeed RT-qPCR analysis showed five- to sixfold augmentation in Kv1.3 mRNA level by LPS in control ($P = 0.014$) and $GR^{LysMCre}$ microglia ($P = 0.049$). Dexamethasone treatment completely repressed this increase in control but not $GR^{LysMCre}$ microglia (Figure 5c).

Microglial GR regulates *in vivo* and *in vitro* Toll-like receptor 4 (TLR4)-initiated innate immune-responsive genes. To examine whether exacerbated inflammatory damage observed in $GR^{LysMCre}$ mice resulted from

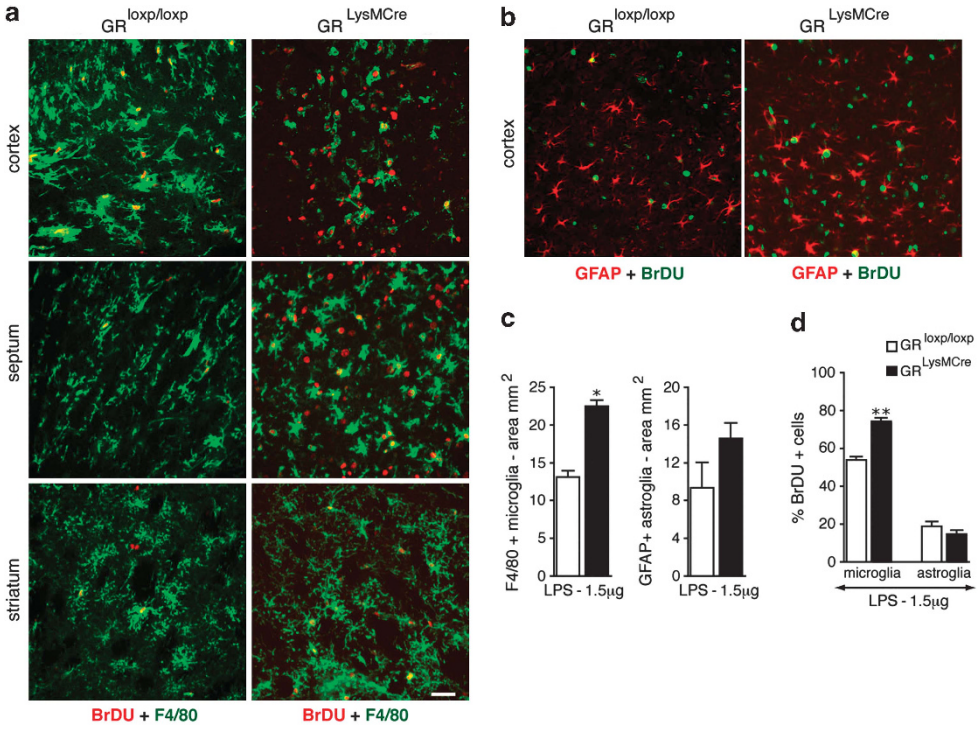

Figure 3 Microglial and astroglial activation and proliferation following intraparenchymal injection of LPS in control and $GR^{LysMCre}$ mice. The activated microglia and astroglia were observed on ipsilateral side of LPS injection. (**a**) Confocal micrographs of F4/80-BrDU double immunofluorescence labeling in the cortex, septum and the striatum. In the cortex of $GR^{LysMCre}$ mutant mice, amoeboid/ macrophagic morphology at the site of injection is observed. (**b**) Confocal micrographs of GFAP-BrDU double immunofluorescence labeling in the cortex. (**c**) The area covered by activated microglia and astroglia analyzed in sections processed for DAB IHC of control and $GR^{LysMCre}$ mice 3 days after 1.5 $\mu g/\mu l$ LPS injection. (**d**) BrDU + microglia and astroglia in control and $GR^{LysMCre}$ mice, showing increased microglial proliferation in $GR^{LysMCre}$ mutants compared with control mice. The values represent mean ± S.E.M., $n=4$. $^{**}P \leq 0.02$, $^{*}P \leq 0.05$ control *versus* $GR^{LysMCre}$ mice

modulations in inflammatory gene expression, mRNA levels of inflammatory genes were analyzed by RT-qPCR in lesioned cortical and striatal areas 6 and 24 h after intraparenchymal LPS injection. An augmentation in the expression of tumor necrosis factor-α (TNFα; $P=0.03$), pro-interleukin-1β (proIL-1β; $P=0.05$) and monocytes chemotactic protein-1 (MCP-1; $P=0.02$) was evident at 24 h in $GR^{LysMCre}$ compared with control mice (Figure 6a). Genes coding for upstream activators of innate immune response, that is, interferon gamma (IFN-γ; $P=0.05$), TLR4 (but not other members of TLR family; $P=0.02$), MyD88 ($P=0.05$) and pro-caspase 4 ($P=0.05$), showed an early increase at 6 h in the lesioned side of $GR^{LysMCre}$ mutants mice compared with control mice (Figure 6b). This indicates that GR rapidly exerts an important regulatory control on these upstream mediators that would otherwise amplify and prolong the inflammatory process.

To verify that microglial GRs are the direct regulators of these pro-inflammatory genes, we analyzed their expression levels in primary microglia cultures following LPS or LPS + dexamethasone treatments. In control but not in $GR^{LysMCre}$ microglia, dexamethasone inhibited mRNA levels of TNF-α, cyclooxygenase-2 (COX-2), inducible nitric oxide synthase (iNOS) and proIL-1β indicating that GR regulates their transcription (Figure 6c). The rise in expression of chemoattractant MCP-1 and chemotactic CXCL-10/IP10 by LPS was also inhibited by dexamethasone in control but not mutant microglia (Figure 6c). In contrast to dexamethasone, aldosterone (50 nM) decreased TNF-α and MCP-1 levels in mutants indicating that MR remains functional in the absence of microglial GR.

Microglial activity and levels of purinergic P2 and adenosine receptor subtypes can alter dramatically in response to neuronal damage. These receptors profoundly affect inflammation by regulating microglial proliferation, process motility, migration, phagocytosis and release of cytokines and chemokines.[27–30] RT-qPCR analysis did not reveal any differences in P2 × 4, P2 × 7, P2Y6 and P2Y12 receptors between control and mutant microglia (data not shown). LPS significantly upregulated adenosine 2A receptors in control but not mutant cultures indicating that GR is involved in expression of this primary anti-inflammatory gene (Figure 6c).

To check whether GR acts to modulate transcription of these genes through suppression of AP-1 and NF-κB transcriptional activities, microglia were transfected with pGL3 piNOSm-luc expression plasmid under the control of iNOS promoter encompassing AP-1 and NF-κB sites. The results of LPS ± dexamethasone treatment of transfected cultures showed an inhibition of luciferase activity by dexamethasone in control but not mutant cultures (Figure 6d).

Analysis of role of microglial GR in priming microglia during chronic unpredictable mild stress (CUMS) and in aging. GC-GR are reported to affect microglial 'priming'

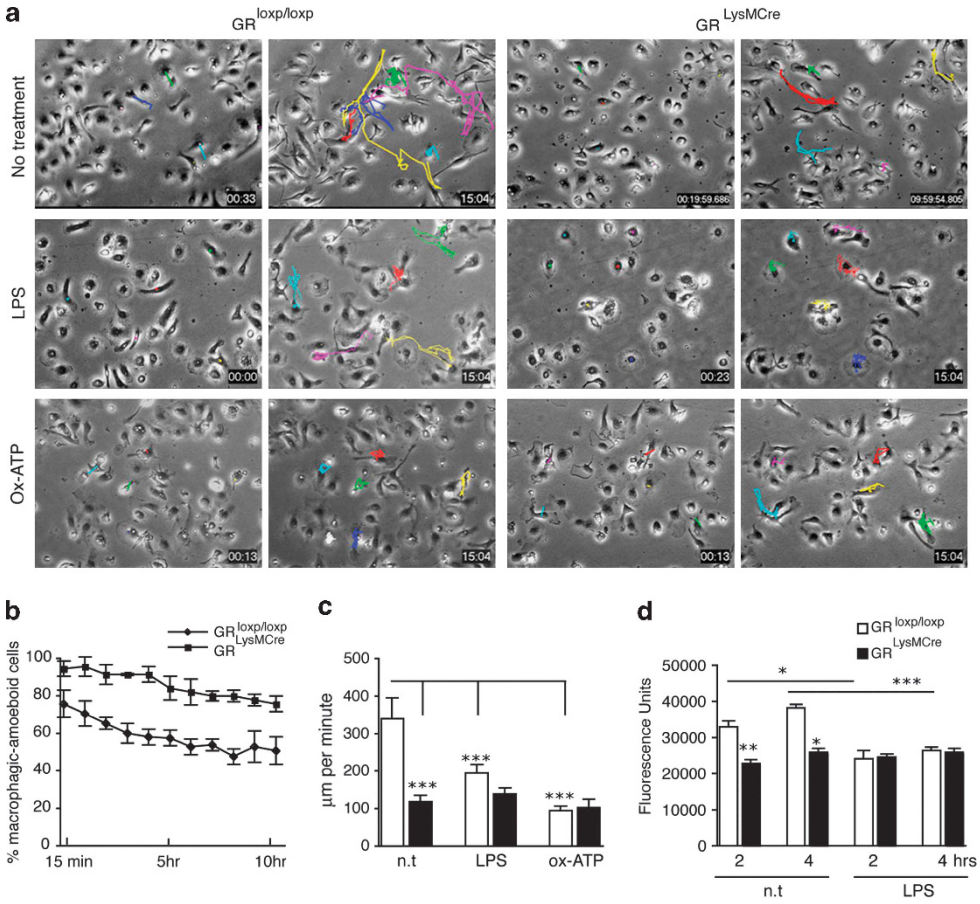

Figure 4 *In vitro* analysis of the microglial morphology and motility in primary microglia cultures prepared from P1 control and $GR^{LysMCre}$ pups. (**a**) Representative examples of time-lapse video microscopy frames from the beginning until the end of recording of cortical microglia cultures prepared from control and $GR^{LysMCre}$ pups, not treated (NT), treated with LPS or ox-ATP. (**b**) Quantification of microglial cells from control and mutant pups displaying amoeboid morphology at indicated time points. The microglial cells constantly change their shape from tubular unipolar, bipolar and tripolar shape to amoeboid macrophagic morphology, however, the changes were less frequent in mutant cells. (**c**) Quantification of cell motility per condition in frames as depicted in **a**. (**d**) Equal numbers of control and mutant microglial cells pre-labeled with DilC fluorescence dye were incubated or not with LPS in FluoroBlok inserts. The cell migration through the inserts was measured at 2 and 4-h time points with bottom fluorescence Spectramax microplate reader. All quantification results are mean ± S.E.M. of three separate experiments. ***$P \leq 0.001$, **$P \leq 0.02$, *$P \leq 0.05$

following stress or in aging,[5,16,18,31–37] thus we tested the role of microglial GR in these two processes. CUMS paradigm alone did not induce neuronal degeneration in young control or mutant mice (data not shown). Following intrastriatal LPS injection 24 h after CUMS in control mice, degenerating neurons in cortex and striatum increased two- to threefold ($P = 0.008$), suggesting microglial sensitization by stress. In mutant mice, this effect was exacerbated because the number of degenerating neurons tripled compared with similarly treated controls ($P = 0.03$, Figure 7a). Corticosterone levels after CUMS were similar between control and mutant mice indicating that increased neuronal death in mutants is unrelated to stress-induced GC levels (Figure 7b *cf.* Figure 1c for mean basal levels). Neuronal degeneration was also analyzed in aged (15–24 months) mice after intrastriatal LPS injection. Old control mice showed greater neuronal degeneration compared with young mice ($P = 0.025$, Figure 7a), and like stressed mutants there was a further significant increase in old $GR^{LysMCre}$ mice ($P = 0.05$, Figure 7a). Lesion volume was increased in both genotypes ($P = 0.03$, control and mutants) after CUMS paradigm and LPS injection, with greater damage in mutants ($P = 0.05$, Figure 7c). In contrast, aging had no influence on cellular damage induced by LPS, the total volume of cellular lesion for each genotype being similar between young and aged animals (Figure 7c). However, old mutants exhibited more damage compared with old controls ($P = 0.03$). These results indicates that stress, as opposed to aging, also affects cells other than microglia and neurons.

Quantification of hypertrophied microglia in cortex and striatum after CUMS showed no difference between controls and mutants. (Figure 7d). As the number of hypertrophied microglia was negligible in cortical/striatal regions of aged mice, they were injected i.p. with LPS (0.5 mg/kg) and killed 24 h later. The mean microglial surface area in the cortex was same between genotypes (Figure 7e). The microglial density increased in cortex and striatum ($P = 0.05$) after i.p. LPS indicating that peripheral inflammation triggers proliferation of microglia, however, no difference between genotypes was observed (Figure 7f).

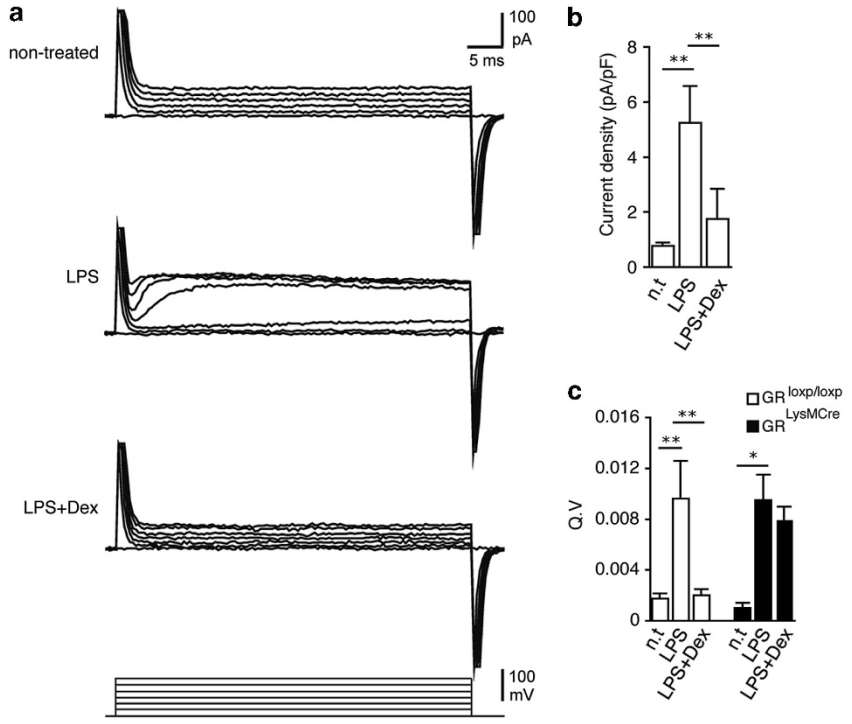

Figure 5 Dexamethasone inhibits the LPS-induced upregulation of delayed rectifier currents in cultured microglia. (**a**) Representative whole-cell membrane currents recorded in microglial cells in response to depolarizing voltage steps from a holding potential of –70 mV (lower traces). The expression of typical delayed rectifier currents in microglia after 6 or 24-h treatment with LPS (100 ng/ml), inhibited when dexamethasone (100 nM) was applied 1 h before and during the LPS treatment. (**b**) Average current densities induced by a voltage step to -10 mV in microglial cells in control conditions ($n=6$), after LPS treatment ($n=7$) and after LPS and dexamethasone co-treatment ($n=6$). $^{**}P \leq 0.02$. (**c**) RT-qPCR analysis of $K_v1.3$ mRNA levels in micorglial cultures from control and $GR^{LysMCre}$ pups; not treated (NT) or treated with LPS (100 ng/ml) or with LPS + dexamethasone (100 nM). Note that LPS significantly induces Kv1.3 mRNA level and that this upregulation is dexamethasone sensitive. In $GR^{LysMCre}$ cultures, dexamethasone does not inhibit Kv1.3 upregulation indicating that the inhibition is GR mediated. $^{**}P \leq 0.02$, $^{*}P \leq 0.05$ NT *versus* LPS treatment

Discussion

Signaling between the immune, endocrine and nervous systems contributes to restoration of homeostatic state following an inflammatory insult. Inappropriate reaction of these systems results in an exaggerated inflammatory response that can trigger neuronal injury and cell death.[6] We have examined the regulation of microglial properties by GR during LPS-induced inflammation using mice inactivated for GR gene in macrophages/microglia. In brain, microglia are the principal TLR4-expressing innate immune cells and thus constitute the main effectors of LPS-induced inflammatory response.[38,39] Intraparenchymal LPS injection triggered a localized inflammatory response characterized by cellular lesion and significant glial activation along the trajectory of injection. The lesion observed in cortex and corpus callosum is likely the result of leakage back along the injection tract and intriguingly, as also reported by Nadeau and Rivest[14] the lesion was less evident in the striatum than in the cortex. It is possible that blood-born monocyte infiltration had occurred at the surface of cortex and/or there are functional differences in microglia between these two regions.[1,40] No difference was found in lesions between control and mutant mice after saline injection. However, following LPS injection, mutants displayed significantly greater cellular lesion, demyelination and damage in the corpus callosum, the latter indicating that GR in white matter microglia prevents pro-inflammatory mediators from injuring axons. LPS induced significant neuronal degeneration in $GR^{LysMCre}$ but not control mice. The most likely explanation of our observations in mutants is the absence of microglial GR brake on inflammation. However, inactivation of GR may alter the expression of other steroid receptors with deleterious effects.[41] We did not observe any difference in the MR expression after LPS injection between control and mutant mice. It is nevertheless possible that MR is active in microglia and exerting pro-inflammatory effects. In this regard, in an experimental model of cerebral ischemia, conditional inactivation of MR in macrophages/microglia resulted in reduced infarct volume[12] indicating important pro-inflammatory activity of MR in these cells.

The result showing greater cellular damage in $GR^{LysMCre}$ mice by LPS after pre-treatment with RU486 at two different time points implies a cross-talk regarding the regulation of inflammatory processes and/or cell survival involving microglial GR and GR in other cells. Within the time period studied, the results using GR^{LckCre} mice showed that GR in T cells does not contribute to inflammatory lesion. Microglial-secreted cytokines, for example, TNF-α or IL-1β, are known to activate astrocytes that can participate in inflammatory response, particularly TLR4 activation by LPS.[42] This raises the possibility that on global inhibition of GR, astrocytes in mutants become more pro-inflammatory. As pro-survival role

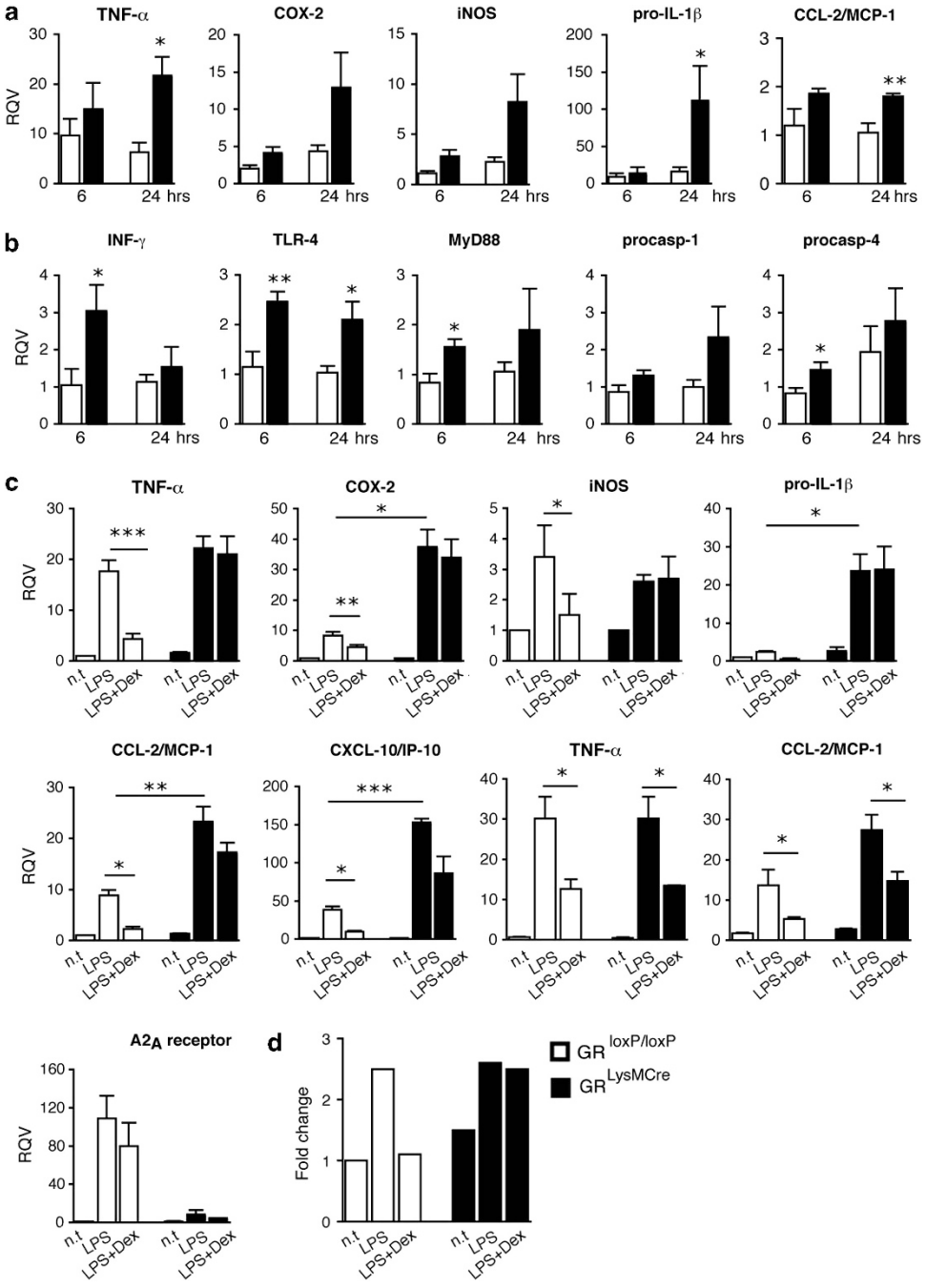

Figure 6 *In vivo* and *in vitro* analysis of changes in inflammatory gene levels after LPS treatment in control and GR^{LysMCr} mice. (**a**) RT-qPCR results of relative changes in the levels of pro-inflammatory mediators TNF-α, iNOS, COX-2 and proIL-1β, MCP-1 in controls and mutants in lesioned cortex-striatal area 6 and 24 h following intraparenchymal LPS injection. PCR values are presented as relative quantitative values (RQV) using HPRT gene as internal control. Increased levels are observed in mutants compared with controls at 24-h time-point. (**b**) RT-qPCR results of upstream activators of innate immune response in $GR^{LysMCre}$ mutants compared with controls 6 and 24 h following intraparenchymal LPS injection. Increased expression in mutants compared with controls is observed at an early time point of 6 h. $^{*}P \leq 0.05$, $^{**}P \leq 0.01$, control *versus* $GR^{LysMCre}$ mutant LPS-injected mice. $n =$ 4–5. (**c**) *In vitro* RT-qPCR analysis of inflammatory gene levels in microglial cultures prepared from P1 cortex of control and $GR^{LysMCre}$ pups. NT $=$ not treated, treated with LPS, LPS $+$ dexamethasone or LPS $+$ aldosterone. β-Microglobulin gene was used as internal control. Note that the expression of proIL-1β, CCL-2 and CXCL-10 is higher in LPS treated $GR^{LysMCre}$ cultures compared with similarly treated control cultures. $^{*}P \leq 0.05$, $^{**}P \leq 0.02$, $^{***}P < 0.001$ $GR^{LysMCre}$ control *versus* mutant cultures, $n = 3$–4 independent experiments. (**d**) Luciferase reporter activity in control and mutant microglial cultures co-transfected with plasmids pGL3-iNOSm-luc and p*Renilla*-TK-luciferase and subsequently treated with LPS or LPS plus dexamethasone. The luciferase luminescence values were normalized with respect to *Renilla* luminescence. The data are presented as fold changes from two independent experiments

of GC-GR has been reported in oligodendrocytes,[43] it is also likely that these cells are susceptible to RU486 pre-treatment and are lost in greater numbers in mutants.

Inflammatory reactions mediated by microglia are characterized by production of both pro-inflammatory and anti-inflammatory factors that determine either neurotrophic or

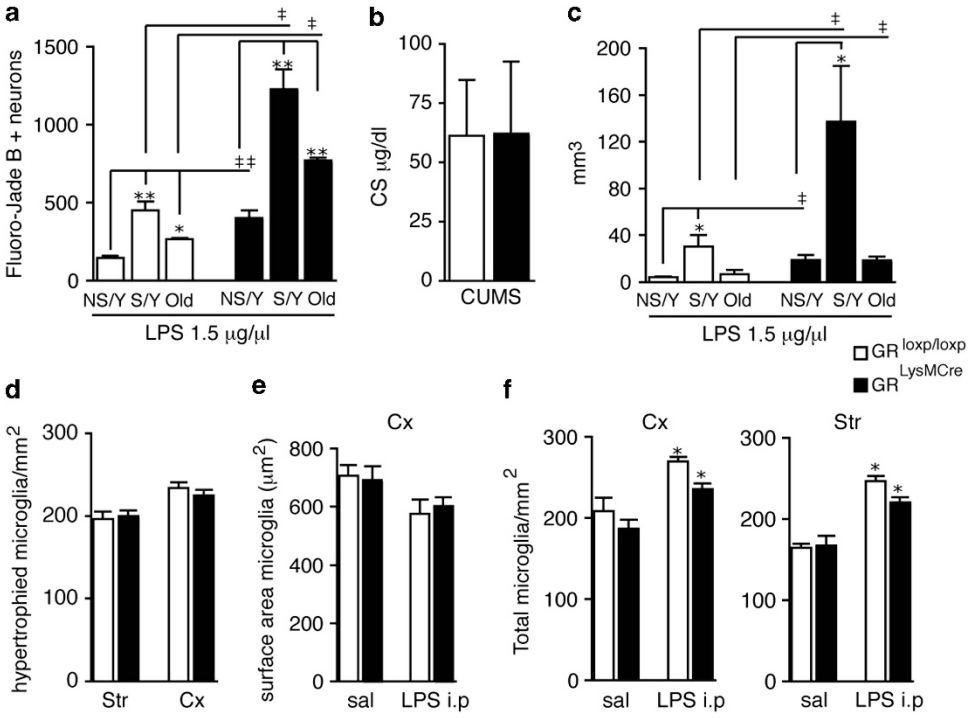

Figure 7 Stress and age-related changes in control and $GR^{LysMCre}$ microglia and its impact on cellular injury induced by LPS. (**a**) Quantification of Fluoro-Jade B + cells 3 days after intraparenchymal injection of LPS in non-stressed young (NS/Y), stressed young (S/Y) and old control and $GR^{LysMCre}$ mice. (**b**) Systemic corticosterone levels in CUMS mice measured 24 h following the end of treatment, $n = 7$–10. (**c**) Quantification of total lesion by cresyl violet staining following LPS injection either in young mice that had undergone CUMS or in old mice. $^{*}P \leq 0.05$, $^{**}P \leq 0.02$ CUMS or aging for each genotype; $^{\ddagger}P \leq 0.05$, $^{\ddagger\ddagger}P \leq 0.02$ mutant *versus* control mice. (**d**) Quantification of hypertrophied microglia in striatum (Str) and cerebral cortex (CX) following CUMS. (**e**) Quantification of microglial size (surface area) in cortex of old control and old mutant $GR^{LysMCre}$ mice, i.p. injected with saline or LPS (0.5 mg/kg). (**f**) Microglial density in cortex (Cx) and striatum (Str) in old $GR^{loxp/loxp}$ and $GR^{LysMCre}$ mice $^{*}P \leq 0.05$, LPS *versus* saline. $n = 4$

neurotoxic outcomes.[3,44–48] *In vivo* results showed a significant rise of pro-inflammatory TNF-α, proIL-1β, iNOS, MCP-1 and COX-2 mRNA levels 24 h following LPS injection in $GR^{LysMCre}$ mice, the results of primary microglial cultures validated that these inflammatory mediators are regulated by microglial GR. Interestingly, we also observed an increased expression of TLR4, MyD88, pro-caspase 4 and IFN-γ levels at 6 h *in vivo* in $GR^{LysMCre}$ mice indicating a positive feed-forward mechanism amplifying the TLR4 signaling pathway in mutants.

We show that GR regulates microglial proliferation, differentiation and motility. Analysis of microgliosis and astrogliosis after an intraparechymal LPS injection revealed an increased spread of activated microglia in the striatal region and overall greater proliferation in mutants compared with controls. In addition, numerous amoeboid-shaped microglia in the cortical surface were observed in $GR^{LysMCre}$ mice. *In vitro*, microglia do not exhibit the morphological 'resting' phenotype observed *in vivo* with small cell soma and many processes and are regarded as 'semi-activated'. The quantification of video-microscopic images *in vitro* showed greater number of amoeboid-shaped microglia in mutant microglial cultures. Moreover, the cell motility analyses showed that mutant microglia without any treatment exhibit decreased cell motility resembling control cultures treated with LPS. These *in vitro* data thus imply activation of GR in microglia during the 12 -day culture period by GC hormone (e.g., present likely in fetal calf serum) leads to down-regulation of some of the features of microglial activation. One interesting finding was the dexamethasone sensitivity of the delayed rectifier currents generated on microglial activation by LPS. $K_v1.3$ potassium channel that mediates the outward currents has been linked to microglial proliferation, peroxynitrite production and respiratory burst.[23,26]

Different types of stressors have been found to 'prime' microglia such that subsequent insult exacerbates microglial inflammatory phenotype resulting in increased lesion and neuronal death.[49–51] Microglial sensitization is also described in aging that may be related to alterations in HPA axis as well as immune deregulation leading to an increased circulating pro-inflammatory cytokines. GC-GR has been implicated in augmenting pro-inflammatory microglial responses either directly or via upregulation of glutamate NMDA receptors.[16,18,35–37] Our results on increased neuronal degeneration in control CUMS mice following LPS injection indicate that microglia become harmful to neurons after stress. Neuronal degeneration was also significantly greater in old compared with young control mice. Mutant mice showed further increase in neuronal degeneration and cellular lesion on intrastriatal LPS injection. If GR in microglia was priming microglia leading to exacerbated damage after stress or in aging, we should not have observed increased damage in mutants after LPS-triggered inflammation. Our results, however, indicate that stress or aging synergize with LPS in

inflicting damage to neuronal and non-neuronal cells and microglial GR acts to limit the damage caused by LPS. In support of this notion, analysis of microglial density or surface area in both stress and aging paradigm did not reveal any differences between control and mutant mice. Thus, it remains to be determined whether GR in other cells types acts on microglial sensitization process during stress and aging.

In conclusion, GR regulates key microglial properties during inflammation, having a determining role in neuronal survival.

Materials and Methods

Mice

Mice with conditional inactivation of GR gene: The $Nr3C1^{loxp/loxp}$;$LysM^{Cre/+}$ (thereafter denominated $GR^{LysMCre}$) and $Nr3C1^{loxp/loxp}$;Tg:LckCre (thereafter denominated GR^{LckCre}) mice were generated by crossing $Nr3C1^{loxp}$ mice[52] with LysMCre and LckCre transgenic mice, which express Cre recombinase inserted by homologous recombination under the lysozyme M promoter gene or Lck-Cre transgene, respectively.[53] The mice were backcrossed to C57BL/6J for at least 10 generations.

Mice were group-housed under a controlled photoperiod (12-h day–night cycles), at constant room temperature (22 °C) and had access to food and water *ad libitum*. Both $GR^{LysMCre}$ and GR^{LckCre} mice were genotyped for the presence of $Nr3C1^{loxp}$ allele and Cre transgene by PCR.[9] All studies were performed in accordance with the Guidelines of the European Convention for the protection of Vertebrate Animals used for Experimental and other scientific purposes of the Council of Europe of 2006, the Helsinki Declaration.

Stereotaxic LPS injections: For stereotaxic surgery, $GR^{LysMCre}$ or GR^{LckCre} mutant mice and $GR^{loxp/loxp}$ control littermates were anesthetized by an i.p. injection of avertin at a dose of 0.5 mg/g. The scalp was shaved and a small hole was made at the surface for injection into the right striatum using the following stereotaxic co-ordinates in mouse Paxinos atlas (David Kopf instruments, Tujunga, CA, USA) from Bregma +1.3 mm anteroposterior, +2 mm lateral and –2.9 mm dorsoventral. In all, 1.5 μg/μl LPS (LPS *Escherichia coli,* serotype 055:B5; Sigma, St Quentin Fallavier, France) dissolved in PBS was injected using 10 μl Hamilton syringe into the right striatum over a 5-min period.

I.p. RU486, BrDU and LPS treatments: $GR^{LysMCre}$ mutants and control mice were pre-treated by an i.p. injection of 30 mg/kg RU486 dissolved in 1 : 9 ethanol:oil or 100 μl ethanol:oil as vehicle 16 or 4 h before stereotaxic injection of LPS. To examine for glial proliferation, the mice were injected i.p. with 50 mg/kg BrdU (Sigma-B5002, St Quentin Fallavier, France) once every 24 h during 3-day period starting immediately after stereotaxic injection of LPS. In experiments on the effects of systemic LPS injection on microglial reactivity, old (15–30 months of age) mice were injected i.p. with a low dose of 0.5 mg/kg LPS or saline vehicle and killed 24 h after.

Chronic unpredictable mild stress paradigm: Chronic variant stress was adapted from stress paradigm described in de Pablos *et al.*[16] $GR^{LysMCre}$ and control mice were exposed to variant-stressor paradigm for 6 consecutive days followed by stereotaxic LPS injection or mock injection on the seventh day. The following paradigm was used: day 1 – food deprivation for 24 h, day 2 – water deprivation for 24 h, day 3 – dirty bedding for 24 h, day 4 – acute restraint at room temperature for 2 h, day 5 – acute restraint at 4 °C, day 6 – cages at an angle for 24 h. Where appropriate the application of stress was performed at different times to minimize predictability.

Analysis of corticosterone levels: Blood from $GR^{LysMCre}$ mice and their control littermates was collected by decapitation between 0700 and 0900 hours. The blood was centrifuged, the plasma stored at –80 °C until analysis. Corticosterone levels in plasma were determined by radioimmunoassay kit (Immunochem TM Corticosterone – MP Biomedicals, Illkirch, France).

Tissue preparation and specific staining. Three days (unless specified) after stereotaxic injections of LPS the mice were anesthetized with CO_2 and rapidly perfused transcardially with ice-cold 0.1 M sodium phosphate buffer (PBS) followed by ice-cold 4% paraformaldehyde in 0.1 M sodium phosphate buffer (PFA). Brains were rapidly removed and post-fixed for 24 h in PFA 4%. In all, 30 μm thick coronal sections were cut serially and stored in PBS containing 0.1% sodium azide. Sections, 180 μm interval, at the level of the lesion were stained for: (i) LFB staining (1% LFB, 95% ethanol, 0.05% acetic acid) for 6 h at 56 °C, followed by 95% ethanol, 0.05%, lithium carbonate and 70% ethanol rinses; (ii) cresyl violet staining (0.5% cresyl violet, 0.3% acetic acid during 2 min, followed by dehydration; and (iii) Fluoro-Jade B (Histo-Chem Inc., Jefferson, AR, USA) as described elsewhere.[54]

Immunostaining: For DAB labeling, the sections were rinsed in PBS, treated with 0.3% H_2O_2 /PBS for 15 min and blocked in 4% new goat serum (Sigma) in PBS-T (PBS/0.3% Triton X-100). They were incubated with 1/750 anti-rabbit ionized calcium binding adaptor molecule 1 (Wako Chemicals GmbH, Neuss, Germany) or 1/1000 GFAP (Sigma) for 48 h at 4 °C. Following incubation with appropriate biotinylated secondary antibodies, the labeling was revealed using avidin–biotin peroxidase ABC kit (Vectastain, Vector Labs, Burlingame, CA, USA). Sections were dehydrated in graded ethanol series and xylene before being coverslipped.

For double-immunofluorescence, the sections were incubated with rabbit anti-GFAP as above and with 1/400 rat anti- F4/80 antibodies (AbD Serotec, Colmar, France). For GR co-expression experiments, they were incubated with: (a) 1/400 mouse anti-NeuN (Cell Signaling, Ozyme, St. Quentin Yvelines, France) and 1/1000 rabbit anti-GR (M-20 Santa-Cruz Biotechnology, Inc., Dallas, TX, USA), (b) rabbit anti-GFAP and 1/500 mouse anti-GR (3D5 AB9568, Abcam, Paris, France), (c) 1/500 rabbit anti-oligodendrocyte transcription factor 2 (Abcam) and mouse anti-GR at 4 °C for 48 h. Following incubation with 1/400 anti-rabbit cyanin-3 (Vector Labs) and 1/400 anti-rat Alexa 488 (Molecular Probes, Life Technologies, In Vitrogen, St. Aubin, France) secondary antibodies and PBS washes, the sections were mounted using vectashield (Vector Labs). For double-immunofluorescence with BrdU, the sections were first denatured in 2 N hydrochloric acid at 37 °C and neutralized with borate buffer. They were blocked in 0.25% gelatin/PBST and incubated with 1/200 mouse anti-BrdU (ImmunologicalsDirect.com, Oxford, UK) antibody followed by incubation with either anti-GFAP or anti-F4/80 antibodies. This was followed by incubation with secondary antibodies: for GFAP-BrDU anti-mouse Alexa 488 and anti-rabbit cyanin-3 antibodies were used whereas for F4/80-BrDU the sections were first incubated with 1/500 anti-mouse biotinylated antibody followed by incubation with 1/500 streptavidin-Alexa Fluor 546 (Molecular Probes) and 1/500 anti-rat Alexa 488 antibodies.

Quantification of the lesion, cell count, fluorescence microscopy and confocal analysis. Cresyl violet-stained sections were used to quantify total lesion volume whereas LFB sections were used for measuring corpus callosum lesion as previously published.[55,56] Briefly, by bright-field microscopy (Nikon, Champigny Sur Marne, France), the lesioned region showing an absence of cresyl violet or LFB staining was delineated for each section. The total area and volume were determined using Mercator image analysis software (Explora Nova, La Rochelle, France). Fluoro-Jade B-positive cells were quantified from photomicrographs taken using FITC filter and ×4 objective (Nikon). For all quantifications related to activated microglia and astroglia, DAB-labeled sections were used. ImageJ software (NIH, USA) was used for quantification of Fluoro-Jade B-positive neurons, microglial and astroglial densities as well as microglial surface area. The genotype of mice was unknown to the investigator at the time of quantification. The double-immunofluorescence labeling of BrDU in microglia or astroglia was analyzed using Leica TCS SP2 confocal microscope (Leica Microsystems, Nanterre, France) in striatal, septal and cortical regions. Analysis was carried out on at least three fields for each region and all the sections (every 180 μm) showing lesions, four animals per group. Confocal images were taken of series range for each field in the section by determining an upper and lower threshold using the Z/Y position obtained from a Spatial Image Series setting. Over the stacks of the images comprising between 4 and 6 μm, GFAP-BrdU-positive and F4/80-BrdU-positive cells were quantified using LCS Lite software (Leica Microsystems) making sure that no overlap of cells occurred in the image series quantified. The double-labeled cells quantified in each region and sections were pooled for each animal.

***In vitro* experiments on primary microglial cells from P1 control and $GR^{LysMCre}$ pups.** Cerebral hemispheres were dissected and cortex extracted from newborn mice after removal of meninges. After dissociation and homogenization, cells were seeded at 0.3×10^6 cells/ml in DMEM containing 10% heat-inactivated FCS. Medium was changed at days 1 and 3, and microglial cells were collected at day 12 by shaking culture dishes to detach cells adhering to the astrocyte monolayer, as described.[57]

For time-lapse video microscopy studies, freshly collected microglia were seeded in DMEM containing 4% FCS. After 90 min of incubation at 37 °C, the video microscopy recording was started, with cells under different treatments: 100 ng/ml LPS, 300 μM oxidized ATP (ox-ATP) or without treatment. The 12-well culture dish was imaged in a 37 °C heated chamber, with 5% CO_2. The images were captured every 10 min using Leica DM IRBE microscope and camera. The treatments were initiated at the start of recording. For FluoroBlok cell migration assays, equivalent control and mutant microglia cells (10 000 per insert) were labeled with 10 μg/ml $DiIC_{12}$ (3) fluorescent dye according to the manufacturer's instructions (BD Biosciences, Le Pont de Claix, France), washed in PBS and resuspended in DMEM medium containing 0.5% FCS and carefully seeded onto 24-multi-well FluoroBlok inserts (8 μm pore size, BD Biosciences). The LPS treatment was initiated and cells incubated at 37 °C. At 2 and 4 h, bottom fluorescence was measured at 549 (absorbance)/565 (emission) nm using SpectraMax M4 multi-mode microplate reader (Molecular Devices, St. Grégoire, France).

For qPCR studies, freshly collected microglia were seeded on 24-well plates in DMEM containing 4% FCS. They were treated 48 h later with 100 ng/ml LPS for 40 min and/or 100 nM dexamethasone, 50 nm aldosterone in DMEM medium containing 0.5% FCS. The cells were pre-treated with either dexamethasone or aldosterone for 1 h. Microglial cells were collected in RLT buffer from RNeasy Mini Kit (Qiagen, Courtaboeuf, France) and stored at -80 °C for total RNA extraction.

RT-qPCR analysis. Six or 24 h after LPS stereotaxic injection, the ipsilateral lesioned and contralateral non-lesioned striata and cortical regions were rapidly punched at -5 to -10 °C and placed in RNA Later (Qiagen). Total RNA was prepared using RNeasy lipid mini kit (Qiagen). The RNA integrity and concentration was determined by using Agilent gel and Agilent apparatus (Agilent Technologies, Les Ulis, France), on average the RIN values were between of 8 and 9. In all, 1 μg of total RNA from whole tissue and 500 ng from cell cultures were used for cDNA synthesis with Superscript III (In Vitrogen, St. Aubin, France). qPCR experiments were performed in triplicates for each condition using Syber Green master mix. HPRT and β-microglobulin primers were used as internal controls for whole tissues and *in vitro* microglial cultures, respectively.

Electrophysiology. Microglial cells grown on glass coverslips were placed in a recording chamber on the stage of an upright microscope (Olympus BX51, Rungis, France) and constantly perfused at room temperature (22–24 °C) at 4 ml/min with an extracellular solution containing (in mM): 126 NaCl, 2.5 KCl, 1.25 NaH_2PO_4, 26 $NaHCO_3$, 20 glucose, 2 $CaCl_2$ and 1 $MgCl_2$, bubbled with carbogene (pH 7.4, 310 mOsm). Whole-cell recordings were performed with pipettes (5–7 MΩ) filled with a solution containing (in mM): 132 K-gluconate, 11 HEPES, 0.1 EGTA, 4 $MgCl_2$ (pH 7.35 adjusted with KOH, osmolarity $\sim$300 mOsm). Voltage-clamp recordings were performed using an Axopatch 200B amplifier (Molecular Devices, Sunnyvale, CA, USA). Currents were low-pass filtered at 5 kHz, collected using PClamp 9 (Molecular Devices) at a frequency 10 kHz and analyzed off line using Clampfit (Molecular Devices). During recordings, the series resistance (Rs) was not compensated and was monitored continuously. Recordings were discarded if Rs increased by $>$20%. Hyperpolarizing and depolarizing steps (from –150 to $+$50 mV for 50 ms) were applied from a holding potential of –70 mV to determine I/V relationship of each recorded cell. Membrane input resistance and capacitance of the cells were determined from the current responses to the voltage pulses ranging from –40 to $+$20 mV from the holding potential of -70 mV. Current densities used to quantify the effects of LPS and dexamethasone on delayed rectifier currents were measured after subtracting the leak current determined from the linear portion of the I/V curve. All potentials were corrected for a junction potential of -8 mV. Values are presented as mean ± S.E.M. Statistical significance was tested with Mann–Whitney *U*-test.

Statistical analysis. Data are expressed as mean ± S.E.M. Statistical analysis was performed using Mann–Whitney tests (StatView 5.0 (Cary, NC, USA) or GraphPad Instat software (San Diego, CA, USA)) unless specifically stated. Differences of $P<0.05$ were considered statistically significant; *n* denotes number of animals for *in vivo* studies or number of individual experiments for *in vitro* experiments.

Conflict of Interest

The authors declare no conflict of interest.

Acknowledgements. We thank N Farman and F Jaisser for MR reagents. This work was supported by the Institut National de la Santé et de la Recherche Médicale (Inserm), the Centre National de la Recherche Scientifique (CNRS), Université Marie et Pierre Curie (UPMC), Association France Parkinson (SV), Fondation de France (SV), Agence Nationale de la Recherche – ANR 2010 BLAN 1419 01 (EA). The Audinat lab is affiliated to Paris School of Neuroscience (ENP) and Tronche lab is a member of LabEX Biological Psychiatry.

1. Ransohoff RM, Perry VH. Microglial physiology: unique stimuli, specialized responses. *Annu Rev Immunol* 2009; **27**: 119–145.
2. Hanisch UK, Kettenmann H. Microglia: active sensor and versatile effector cells in the normal and pathologic brain. *Nat Neurosci* 2007; **10**: 1387–1394.
3. Glezer I, Simard AR, Rivest S. Neuroprotective role of the innate immune system by microglia. *Neuroscience* 2007; **147**: 867–883.
4. Rivest S. Regulation of innate immune responses in the brain. *Nat Rev Immunol* 2009; **9**: 429–439.
5. Perry VH, Nicoll JA, Holmes C. Microglia in neurodegenerative disease. *Nat Rev Neurol* 2010; **6**: 193–201.
6. Sternberg EM. Neural regulation of innate immunity: a coordinated nonspecific host response to pathogens. *Nat Rev Immunol* 2006; **6**: 318–328.
7. Sierra A, Gottfried-Blackmore A, Milner TA, McEwen BS, Bulloch K. Steroid hormone receptor expression and function in microglia. *Glia* 2008; **56**: 659–674.
8. Saijo K, Collier JG, Li AC, Katzenellenbogen JA, Glass CK. An ADIOL-ERbeta-CtBP transrepression pathway negatively regulates microglia-mediated inflammation. *Cell* 2011; **145**: 584–595.
9. Ros-Bernal F, Hunot S, Herrero MT, Parnadeau S, Corvol JC, Lu L *et al.* Microglial glucocorticoid receptors play a pivotal role in regulating dopaminergic neurodegeneration in parkinsonism. *Proc Natl Acad Sci USA* 2011; **108**: 6632–6637.
10. Fuller PJ, Yao Y, Yang J, Young MJ. Mechanisms of ligand specificity of the mineralocorticoid receptor. *J Endocrinol* 2012; **213**: 15–24.
11. Usher MG, Duan SZ, Ivaschenko CY, Frieler RA, Berger S, Schutz G *et al.* Myeloid mineralocorticoid receptor controls macrophage polarization and cardiovascular hypertrophy and remodeling in mice. *J Clin Invest* 2010; **120**: 3350–3364.
12. Frieler RA, Meng H, Duan SZ, Berger S, Schutz G, He Y *et al.* Myeloid-specific deletion of the mineralocorticoid receptor reduces infarct volume and alters inflammation during cerebral ischemia. *Stroke* 2011; **42**: 179–185.
13. Goulding NJ. The molecular complexity of glucocorticoid actions in inflammation—a four-ring circus. *Curr Opin Pharmacol* 2004; **4**: 629–636.
14. Nadeau S, Rivest S. Glucocorticoids play a fundamental role in protecting the brain during innate immune response. *J Neurosci* 2003; **23**: 5536–5544.
15. Sugo N, Hurn PD, Morahan MB, Hattori K, Traystman RJ, DeVries AC. Social stress exacerbates focal cerebral ischemia in mice. *Stroke* 2002; **33**: 1660–1664.
16. de Pablos RM, Villaran RF, Arguelles S, Herrera AJ, Venero JL, Ayala A *et al.* Stress increases vulnerability to inflammation in the rat prefrontal cortex. *J Neurosci* 2006; **26**: 5709–5719.
17. Alexander JK, DeVries AC, Kigerl KA, Dahlman JM, Popovich PG. Stress exacerbates neuropathic pain via glucocorticoid and NMDA receptor activation. *Brain Behav Immun* 2009; **23**: 851–860.
18. Munhoz CD, Lepsch LB, Kawamoto EM, Malta MB, Lima Lde S, Avellar MC *et al.* Chronic unpredictable stress exacerbates lipopolysaccharide-induced activation of nuclear factor-kappaB in the frontal cortex and hippocampus via glucocorticoid secretion. *J Neurosci* 2006; **26**: 3813–3820.
19. Wohleb ES, Hanke ML, Corona AW, Powell ND, Stiner LM, Bailey MT *et al.* beta-Adrenergic receptor antagonism prevents anxiety-like behavior and microglial reactivity induced by repeated social defeat. *J Neurosci* 2011; **31**: 6277–6288.
20. Frank MG, Thompson BM, Watkins LR, Maier SF. Glucocorticoids mediate stress-induced priming of microglial pro-inflammatory responses. *Brain Behav Immun* 2012; **26**: 337–345.
21. Njie EG, Boelen E, Stassen FR, Steinbusch HW, Borchelt DR, Streit WJ. Ex vivo cultures of microglia from young and aged rodent brain reveal age-related changes in microglial function. *Neurobiol Aging* 2012; **33**: 195 e191–112.
22. Panda A, Arjona A, Sapey E, Bai F, Fikrig E, Montgomery RR *et al.* Human innate immunosenescence: causes and consequences for immunity in old age. *Trends Immunol* 2009; **30**: 325–333.
23. Kettenmann H, Hanisch UK, Noda M, Verkhratsky A. Physiology of microglia. *Physiol Rev* 2011; **91**: 461–553.
24. Boucsein C, Kettenmann H, Nolte C. Electrophysiological properties of microglial cells in normal and pathologic rat brain slices. *Eur J Neurosci* 2000; **12**: 2049–2058.
25. Menteyne A, Levavasseur F, Audinat E, Avignone E. Predominant functional expression of Kv1.3 by activated microglia of the hippocampus after status epilepticus. *PLoS One* 2009; **4**: e6770.
26. Fordyce CB, Jagasia R, Zhu X, Schlichter LC. Microglia Kv1.3 channels contribute to their ability to kill neurons. *J Neurosci* 2005; **25**: 7139–7149.
27. Di Virgilio F, Ceruti S, Bramanti P, Abbracchio MP. Purinergic signalling in inflammation of the central nervous system. *Trends Neurosci* 2009; **32**: 79–87.

28. van der Putten C, Zuiderwijk-Sick EA, van Straalen L, de Geus ED, Boven LA, Kondova I *et al.* Differential expression of adenosine A3 receptors controls adenosine A2A receptor-mediated inhibition of TLR responses in microglia. *J Immunol* 2009; **182**: 7603–7612.
29. Burnstock G, Krugel U, Abbracchio MP, Illes P. Purinergic signalling: from normal behaviour to pathological brain function. *Prog Neurobiol* 2011; **95**: 229–274.
30. Gessi S, Merighi S, Varani K, Borea PA. Adenosine receptors in health and disease. *Adv Pharmacol* 2011; **61**: 41–75.
31. Jeong YH, Park CH, Yoo J, Shin KY, Ahn SM, Kim HS *et al.* Chronic stress accelerates learning and memory impairments and increases amyloid deposition in APPV717I-CT100 transgenic mice, an Alzheimer's disease model. *FASEB J* 2006; **20**: 729–731.
32. Moreno B, Jukes JP, Vergara-Irigaray N, Errea O, Villoslada P, Perry VH *et al.* Systemic inflammation induces axon injury during brain inflammation. *Ann Neurol* 2011; **70**: 932–942.
33. Aguilera G. HPA axis responsiveness to stress: implications for healthy aging. *Exp Gerontol* 2011; **46**: 90–95.
34. Jurgens HA, Johnson RW. Dysregulated neuronal-microglial cross-talk during aging, stress and inflammation. *Exp Neurol* 2012; **233**: 40–48.
35. Johnson EA, O'Callaghan JP, Miller DB. Chronic treatment with supraphysiological levels of corticosterone enhances D-MDMA-induced dopaminergic neurotoxicity in the C57BL/6J female mouse. *Brain Res* 2002; **933**: 130–138.
36. Rangon CM, Fortes S, Lelievre V, Leroux P, Plaisant F, Joubert C *et al.* Chronic mild stress during gestation worsens neonatal brain lesions in mice. *J Neurosci* 2007; **27**: 7532–7540.
37. Frank MG, Miguel ZD, Watkins LR, Maier SF. Prior exposure to glucocorticoids sensitizes the neuroinflammatory and peripheral inflammatory responses to E. coli lipopolysaccharide. *Brain Behav Immun* 2010; **24**: 19–30.
38. Chakravarty S, Herkenham M. Toll-like receptor 4 on nonhematopoietic cells sustains CNS inflammation during endotoxemia, independent of systemic cytokines. *J Neurosci* 2005; **25**: 1788–1796.
39. Pascual O, Ben Achour S, Rostaing P, Triller A, Bessis A. Microglia activation triggers astrocyte-mediated modulation of excitatory neurotransmission. *Proc Natl Acad Sci USA* 2012; **109**: E197–E205.
40. Lawson LJ, Perry VH, Dri P, Gordon S. Heterogeneity in the distribution and morphology of microglia in the normal adult mouse brain. *Neuroscience* 1990; **39**: 151–170.
41. Bousquet E, Zhao M, Ly A, Leroux Les Jardins G, Goldenberg B, Naud MC *et al.* The aldosterone-mineralocorticoid receptor pathway exerts anti-inflammatory effects in endotoxin-induced uveitis. *PLoS One* **7**: e49036.
42. Holm TH, Draeby D, Owens T. Microglia are required for astroglial Toll-like receptor 4 response and for optimal TLR2 and TLR3 response. *Glia* 2012; **60**: 630–638.
43. Xu L, Xu Z, Xu M. Glucocorticoid treatment restores the impaired suppressive function of regulatory T cells in patients with relapsing-remitting multiple sclerosis. *Clin Exp Immunol* 2009; **158**: 26–30.
44. Chao CC, Hu S, Sheng WS, Tsang M, Peterson PK. Tumor necrosis factor-alpha mediates the release of bioactive transforming growth factor-beta in murine microglial cell cultures. *Clin Immunol Immunopathol* 1995; **77**: 358–365.
45. Streit WJ, Walter SA, Pennell NA. Reactive microgliosis. *Prog Neurobiol* 1999; **57**: 563–581.
46. Vitkovic L, Bockaert J, Jacque C. 'Inflammatory' cytokines: neuromodulators in normal brain? *J Neurochem* 2000; **74**: 457–471.
47. Garden GA, Moller T. Microglia biology in health and disease. *J Neuroimmune Pharmacol* 2006; **1**: 127–137.
48. Simard AR, Rivest S. Neuroprotective effects of resident microglia following acute brain injury. *J Comp Neurol* 2007; **504**: 716–729.
49. Frank MG, Baratta MV, Sprunger DB, Watkins LR, Maier SF. Microglia serve as a neuroimmune substrate for stress-induced potentiation of CNS pro-inflammatory cytokine responses. *Brain Behav Immun* 2007; **21**: 47–59.
50. Sugama S, Fujita M, Hashimoto M, Conti B. Stress induced morphological microglial activation in the rodent brain: involvement of interleukin-18. *Neuroscience* 2007; **146**: 1388–1399.
51. Espinosa-Oliva AM, de Pablos RM, Villaran RF, Arguelles S, Venero JL, Machado A *et al.* Stress is critical for LPS-induced activation of microglia and damage in the rat hippocampus. *Neurobiol Aging* 2009; **32**: 85–102.
52. Tronche F, Kellendonk C, Kretz O, Gass P, Anlag K, Orban PC *et al.* Disruption of the glucocorticoid receptor gene in the nervous system results in reduced anxiety. *Nat Genet* 1999; **23**: 99–103.
53. Tuckermann JP, Kleiman A, Moriggl R, Spanbroek R, Neumann A, Illing A *et al.* Macrophages and neutrophils are the targets for immune suppression by glucocorticoids in contact allergy. *J Clin Invest* 2007; **117**: 1381–1390.
54. Schmued LC, Albertson C, Slikker W Jr. Fluoro-Jade: a novel fluorochrome for the sensitive and reliable histochemical localization of neuronal degeneration. *Brain Res* 1997; **751**: 37–46.
55. Kawano T, Kunz A, Abe T, Girouard H, Anrather J, Zhou P *et al.* iNOS-derived NO and nox2-derived superoxide confer tolerance to excitotoxic brain injury through peroxynitrite. *J Cereb Blood Flow Metab* 2007; **27**: 1453–1462.
56. Capone C, Fabrizi C, Piovesan P, Principato MC, Marzorati P, Ghirardi O *et al.* 2-Aminotetraline derivative protects from ischemia/reperfusion brain injury with a broad therapeutic window. *Neuropsychopharmacology* 2007; **32**: 1302–1311.
57. Meme W, Calvo CF, Froger N, Ezan P, Amigou E, Koulakoff A *et al.* Proinflammatory cytokines released from microglia inhibit gap junctions in astrocytes: potentiation by beta-amyloid. *FASEB J* 2006; **20**: 494–496.

Supplementary Information accompanies this paper on Cell Death and Differentiation website (http://www.nature.com/cdd)